

Influence of the degradation of the organic matrix on the microscopic fracture behavior of trabecular bone

Georg E. Fantner^{a,*}, Henrik Birkedal^b, Johannes H. Kindt^a, Tue Hassenkam^a, James C. Weaver^d, Jacquelin A. Cutroni^a, Bonnie L. Bosma^d, Lukmaan Bawazer^b, Marquesa M. Finch^a, Geraldo A.G. Cidade^a, Daniel E. Morse^d, Galen D. Stucky^c, Paul K. Hansma^a

^aDepartment of Physics, University of California Santa Barbara, CA 93106, United States

^bDepartment of Chemistry and Biochemistry, University of California Santa Barbara, CA 93106, United States

^cDepartment of Chemistry and Biochemistry and Materials Department, University of California Santa Barbara, CA 93106, United States

^dInstitute for Collaborative Biotechnologies, University of California Santa Barbara, CA 93106, United States

Received 16 December 2003; revised 25 May 2004; accepted 27 May 2004

Available online 28 September 2004

Abstract

In recent years, the important role of the organic matrix for the mechanical properties of bone has become increasingly apparent. It is therefore of great interest to understand the interactions between the organic and inorganic constituents of bone and learn the mechanisms by which the organic matrix contributes to the remarkable properties of this complex biomaterial. In this paper, we present a multifaceted view of the changes of bone's properties due to heat-induced degradation of the organic matrix. We compare the microscopic fracture behavior (scanning electron microscopy; SEM), the topography of the surfaces (atomic force microscopy; AFM), the condition of bone constituents [X-ray diffraction (XRD), thermogravimetric analysis (TGA), and gel electrophoresis], and the macromechanical properties of healthy bovine trabecular bone with trabecular bone that has a heat-degraded organic matrix. We show that heat treatment changes the microfracture behavior of trabecular bone. The primary failure mode of untreated trabecular bone is fibril-guided delamination, with mineralized collagen filaments bridging the gap of the microcrack. In contrast, bone that has been baked at 200°C fractures nondirectionally like a brittle material, with no fibers spanning the microcracks. Finally, bone that has been boiled for 2 h in PBS solution fractures by delamination with many small filaments spanning the microcracks, so that the edges of the microcracks become difficult to distinguish. Of the methods we used, baking most effectively weakens the mechanical strength of bone, creating the most brittle material. Boiled bone is stronger than baked bone, but weaker than untreated bone. Boiled bone is more elastic than untreated bone, which is in turn more elastic than baked bone. These studies clearly emphasize the importance of the organic matrix in affecting the fracture mechanics of bone.

© 2004 Elsevier Inc. All rights reserved.

Keywords: Fracture mechanism; Organic matrix; Bone strength; Mechanical properties; Microcracks

Introduction

The mechanisms that form the basis of the mechanical properties of bone and the main failure mechanisms of healthy and diseased bone are of great scientific and medical interest [1–3]. Many investigations have focused on the influence of the microscopic structure of bones on their

mechanical properties [4–10], including studies on stress accumulation and formation of microcracks [11,12]. The structure of bone on the nanoscale is also very important for the mechanical performance of the bone as a whole. Interactions in nanocomposites, such as bone [13], nacre [14], and many others, derive their remarkable properties from the interaction of the organic (proteins, other organic polymers) and the inorganic (crystal) constituents [14–16]. In bone, the main component of the organic matrix is type I collagen and the crystal phase consists mainly of dahllite (carbonated hydroxylapatite) [13]. It has been shown that

* Corresponding author.

E-mail address: fantner@physics.ucsb.edu (G.E. Fantner).

the organic phase in bone has great influence on the mechanical properties of the whole biocomposite [13,17–22]. To understand these mechanical properties, and to predict and prevent bone failure, it is necessary to understand the nanoscale organization of the bone [23–25]; in particular, how the components of the bone matrix interact [22,26] and what role they play in the mechanical properties of the bulk material, as changes in any of the constituents will influence the mechanical properties of the whole composite [18,20,21,27]. To assess the role of the individual constituents for the mechanical strength, we specifically targeted the organic matrix by heat treating the bone samples [28] in different ways (baking and boiling) and looked for changes in their mechanical properties, fracture behavior, and appearance. We investigated microscopic fracture behavior with high-resolution scanning electron microscopy (SEM) [29] and topology with atomic force microscopy (AFM) [30]. The influence of the heat degradation on the individual constituents of bone was assessed by X-ray diffraction [31], gel electrophoresis [32], and thermogravimetric analysis (TGA) [33].

Materials and methods

We investigated trabecular bone from bovine vertebrae. The vertebrae were obtained from a butcher and immediately frozen upon receipt. The bone was cut into $5 \times 5 \times 4$ mm cubes using a regular and a diamond band saw. The marrow was cleaned out using a Water Pik (a high-pressure water jet used for dental hygiene). The samples were then polished with 600-grit sandpaper under flowing water. The samples were always kept moist during these steps and stored, briefly, in 0.1 M phosphate-buffered saline (PBS) between steps.

We studied three types of bone samples [34]:

Untreated “healthy” bone: We extracted trabecular bone from the bovine vertebrae as described above and froze the samples at -20°C typically for not more than 10 days.

Baked bone: The bone samples were heated in a laboratory oven for 40 min at 200°C . Following heat treatment they were rehydrated overnight in PBS before experimental use.

Boiled bone: The bone samples were boiled in PBS solution for 2 h and then frozen (-20°C) until the time of the experiments (typically not more than 24 h). During preparation samples were stored for short periods of time in 0.1 M phosphate-buffered saline (PBS).

We used an FEI (XL 40 Sirion) scanning electron microscope (SEM) to investigate the fracture behavior of the heat treated bone. Samples for scanning electron microscopy (SEM) were typically $5 \times 5 \times 4$ mm in size. They were polished and cleaned with a high-pressure water jet to remove loose residue. The samples were quasi statically compressed (in PBS solution) in a small, SEM compatible vice until a partial fracture of the trabeculae was

observed under a stereo dissecting microscope. The samples were compressed to a strain of approximately 20%. All samples were compressed by the same amount. The samples were then rinsed in deionized water to prevent salt crystallization. The samples were degassed in a vacuum oven (10^{-3} Torr, 30°C) overnight and then gold/palladium coated for SEM imaging. The images presented in Figs. 2–4 are representative figures of features observed on multiple locations (out of 80 locations investigated) on multiple samples (total samples: six untreated, two boiled, two baked).

For AFM sample preparation, the bone cubes were studied under an optical microscope to find single trabeculae that were accessible to the AFM and were not damaged by the cutting. The sample cubes were dried and glued to a steel sample disc using Devcon 2-ton epoxy. Images were recorded in air, at room temperature, with a scan rate of 1 Hz, on a standard tapping mode atomic force microscopy (Digital Instruments Nanoscope IV) using silicon cantilevers with a force constant of approximately 40 N/m and a resonance frequency of 300 kHz (TAP300, NanoDevices). Images shown in this paper are representative of features observed in tens of AFM images.

Trabecular bone samples for gel electrophoresis were cleaned with a pressurized stream of PBS, rinsed with ultra pure water, and lyophilized until dry. The samples were ground with a mortar and pestle to a fine powder and ca. 45 mg of material was suspended in Tris–Glycine SDS sample buffer (Invitrogen, Carlsbad, Ca), reduced with DTT (total sample volume of 120 μl), and heat denatured at 85°C for 20 min. The suspension was centrifuged and the supernatant was loaded on a 4–20% Tris–Glycine SDS PAGE gel and run for 2 h at 125 V. The experiment was conducted five times, each time starting with fresh bone samples. The gels from these measurements all showed the same features.

X-ray powder diffraction data were collected on a Scintag X2 powder diffractometer using $\text{Cu K}\alpha$ radiation from a tube operated at 45 kV and 35 mA. For heated bone, a sample heated to 200°C for 40 min was measured from 20° to $55^{\circ} 2\theta$, where 2θ is the Bragg scattering angle, using a step size of $\Delta 2\theta = 0.02^{\circ}$ and an exposure time of 2.1 s/step. Untreated bone was measured using $\Delta 2\theta = 0.035^{\circ}$ and 11 s/step while a boiled sample was measured using $\Delta 2\theta = 0.02^{\circ}$ and 21 s/step. Since the diffraction peaks are significantly size broadened, the different step size used for the untreated sample does not influence the results. We repeated the experiment on two bone samples per treatment and got equivalent results.

Thermal gravimetric analysis (TGA) was performed using a Netsch STA 409 thermal analyzer. Samples were heated from room temperature to 1100°C at 10 K/min. Samples were extracted from one single vertebrae and divided into two sets: one which was left untreated and the other which was boiled for 2 h in 0.01 M PBS. From each set, at least three TGA runs were performed. This procedure was used to minimize intervertebrae variability

and indeed when considering samples from different specimens a larger spread in weight loss was observed. In Fig. 6B, the data have been normalized to the mass at 234°C, which was determined to be the average crossover temperature from the region dominated by water loss to the region where the organic matrix is lost. For the boiled bone, three samples were run. For the untreated bone, four samples were run. The data curves were averaged for each group. The standard deviation was used as an indicator for sample variation.

Macromechanical testing was performed in a home built compression tester with the capability to load the bone at loading rates comparable to a typical fall on the hip (approximately 15 ms) [35]. The bone samples were mounted in a fluid cell and compressed by an aluminum plunger, see Fig. 1. The plunger was loaded with impacts from a pivoting weight. The impact face of the weight was padded with elastomer to achieve the desired 15 ms rise time to the peak impact force. The rise time to peak force depends on the elastic property of the combination of the bone sample and the elastomer. In our experiments, the rise time to peak force was primarily determined by the elastic modulus of the elastomer since the elastomer has a much lower elastic modulus. Changes in the rise time due to

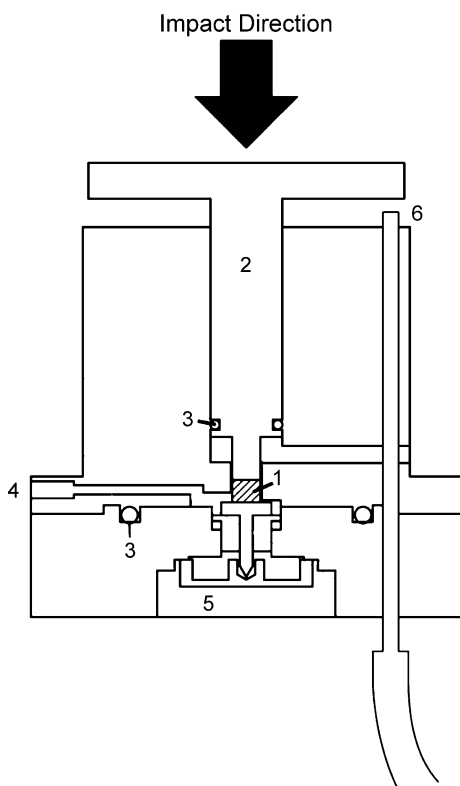


Fig. 1. Bone compression apparatus. Samples (1) are compressed by aluminum plunger (2) in the direction indicated by the arrow. Samples were constantly in liquid (sealed sample chamber; 3) and the liquid could be changed during the experiment through the fluid lines (4). The force that was exerted on the sample was measured with a load cell (5). The compression of the sample was measured by measuring the displacement of the plunger with a fiber optic positioning sensor (6).

different elastic moduli of the bone samples were negligible. Each sample was loaded with a series of impacts following the same protocol for each sample: starting at 0.5 J impacts, the impact energy was increased after each fourth hit to 0.75, 1, 1.25, 1.5, 1.75, 2, 2.5, 3, 3.5, 4, 4.5, 5, 6, 7, 8, 9, and 10 J, respectively. The experiment was aborted when the sample had been compressed by more than 2 mm. The force was measured with a load-cell (LB01K, Transducer Techniques) and the compression of the sample was assessed by measuring the displacement of the plunger with a fiber optic position sensor (MTI 2000, MTI Instruments). The data were collected using LabView 6.0. We tested six samples of untreated bone, six samples of boiled bone, and four samples of baked bone. The sample variation is represented by error bars in Fig. 8A.

Results

Fig. 2 shows SEM images of an untreated bone partially fractured by compression. Fig. 2A shows the bone cracking at stress accumulation points and reveals microcracks within the bulk material. The directions of most of the cracks are parallel to lines of equal stress, resulting in a delamination rather than a cracking normal to the trabecular surface. Examples are shown by the arrows in Fig. 2A. Further magnification of a crack tip (Fig. 2B) shows that there are filaments spanning the gap between the separated pieces. Similar organic filaments have been reported previously to span the cracks in abalone shell, a biocomposite consisting primarily of calcium carbonate and insoluble proteins (e.g., lustrin A). These organic filaments were proven to greatly improve the mechanical strength of the shell [14]. Recently, similar fibers were found in microcracks of cortical bone [22]. Fig. 2C shows a delamination crack in the untreated bone with fibrils spanning the gap over a distance of up to 20 μm (Fig. 2D). The length and width of the fibers indicate that one filament consists of bundles of molecules, primarily collagen [36]. Some of these filaments show the 67-nm banding pattern characteristic of collagen fibrils (data not shown).

Fig. 3 shows SEM images of a baked bone partially fractured by compression. The crack formation is different from the untreated bone. The fracture surfaces are no longer smooth, but are rough and branched. The fractures are not primarily due to delamination and cracks occur in all directions. Figs. 3B and C show two cracks running perpendicularly into each other. In direct contrast to the healthy untreated bone, the microcracks are not spanned by filaments (Fig. 3D).

Fig. 4 shows SEM images of boiled bone partially fractured by compression. Fig. 4B shows a microcrack seen from the surface as well as in the cross section. The fracture is not a single crack but branches into several cracks that form loose bone pieces between the two main fractured surfaces (Fig. 4C). There are many filaments spanning the

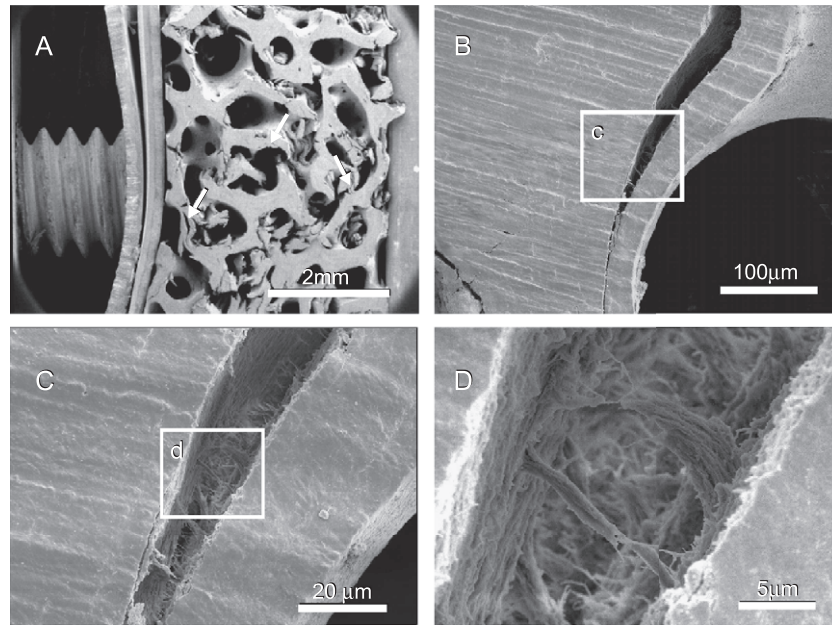


Fig. 2. SEM images of partially crushed, untreated trabecular bone. (A) Low magnification view showing fracture points and small cracks. White arrows point to delamination cracks. (B) View of a crack end, revealing filaments spanning the microcrack. (C) Delamination crack on a polished surface. (D) High magnification view of the crack shows organic filaments spanning the gap in the microcrack over several μm .

crack, making the exact fracture surface difficult to distinguish (Fig. 4D).

The heat treatments not only influence the fracture behavior, but also the appearance of the bone surfaces. Figure 5 shows atomic force microscopy (AFM) images of surfaces of untreated, baked, and boiled bone samples, respectively. The surface of an untreated bone is shown in Fig. 5A. The 67-nm banding pattern that is typical for collagen fibrils is clearly visible [37], the image represents AFM height data. Fig. 5B

shows the surface of a baked bone that still exhibits a fibrous surface. However, the banding pattern observed in the untreated samples has disappeared and the fibers are more distinct. On the surface of the boiled bone, no fibrils are visible (Fig. 5C). The surface appears to be covered with a soft layer, possibly remnants of organic material that might cover underlying fibrils. Several AFM images were taken distributed over each sample. The images shown here appear to be representative for the whole surface of each sample.

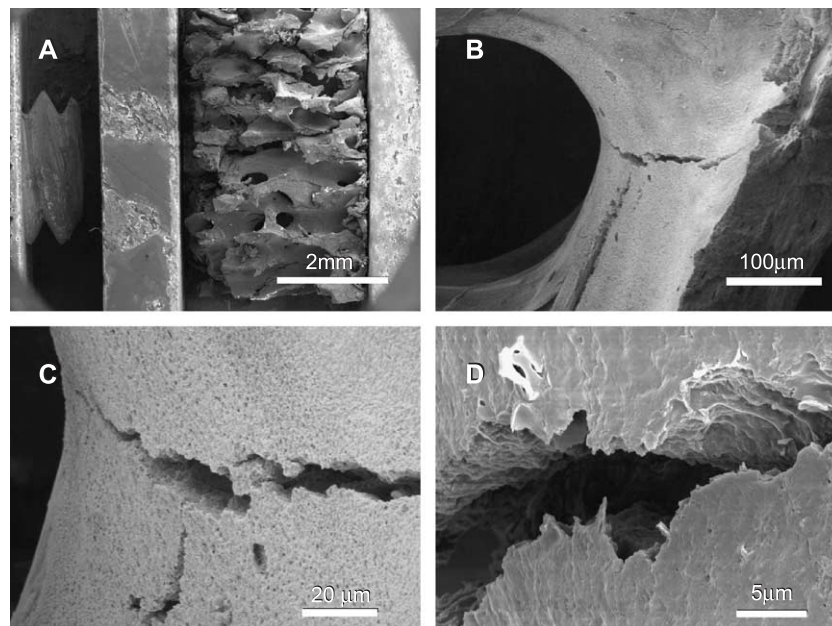


Fig. 3. SEM images of partially crushed, baked trabecular bone. (A) Crack formation on an inside surface of the trabeculae. (B and C) Cracks no longer propagate parallel to lines of equal stress but occur in all directions, even crossing into each other. (D) The microcracks shows no filaments spanning the crack. The surface of the trabeculae has a rough topography.

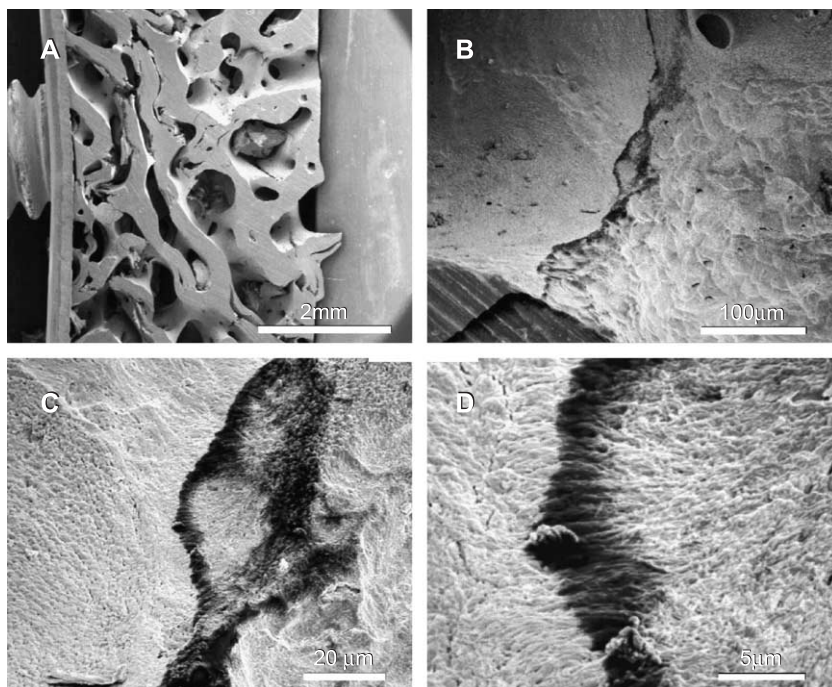


Fig. 4. SEM images of partially crushed, boiled trabecular bone. (A) Low magnification view of the deformed trabeculae. The bone shows less breaks than the untreated or baked bone. (B) A crack formation seen from the surface and from the cross section, showing the multiple cracks that form the fracture. (C and D) High magnification view of the crack. Many filaments span the microcrack. The crack surfaces become hard to distinguish.

To investigate the effects of heating on each constituent phase (organic and inorganic), we looked at the individual constituents and on the weight ratio of the inorganic and organic phase after heat treatment.

X-ray diffraction of the untreated, baked, and boiled bone shows that the heat treatment at these temperatures does not significantly influence the inorganic phase (Fig. 6A). The peaks in the spectrum are nearly identical in peak width (for the 32° peak: $1.68^\circ \pm 0.07^\circ$). The slight variation in relative peak height results from a difference in preferred orientation due to the fact that it was not possible to grind the untreated and boiled bone to a fine powder (this effect was observed in two measurements on two different diffractometers).

Fig. 6B compares thermal gravimetric analysis of untreated and boiled samples extracted from the same

vertebra. The organic material is lost between approximately 250°C and 500°C . Thus, in our samples baked at 200°C for the other experiments, we know that the organic material that is degraded is still present. The degradation of the organic material in the baked samples is shown by a color change from white to light brown, as well as by the gel results discussed below. In the boiled sample, in addition to slight degradation shown by a small color change from white to ivory, there is also some loss of organic material into the solution. There is clearly relatively less organic material in the boiled samples. The average weight fraction of organic, normalized to the 234°C starting mass to eliminate variations due to differences in the amount of water, is 28.9% for the untreated bone and 26.3% for the boiled bone. Comparison of TGA

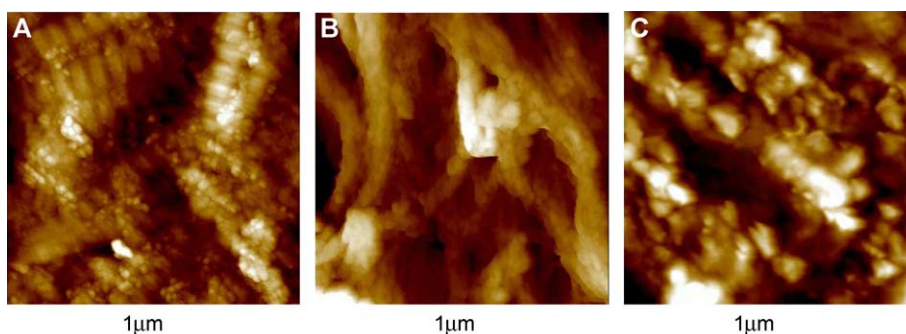


Fig. 5. AFM images of bone surfaces. (A) Untreated bone, showing the 67-nm banding pattern typical to collagen fibrils (image shows sample height). (B) On the surface of baked bone, there is still a fibrous structure, but the collagen banding pattern has disappeared (image shows sample height). This would be consistent with mineralized fibrils degrading to fibers of mineral particles associated with each other and what is left of the degraded collagen, now unbanded, that they previously coated. (C) The boiled surface shows no distinct fibrillar components but appears to be covered with a soft layer, possibly loose organic.

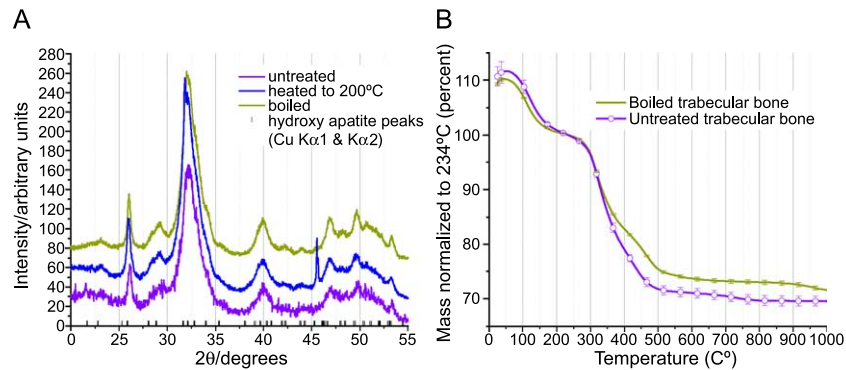


Fig. 6. Influence of the heat treatments on the organic and inorganic components of bone. (A) X-ray diffraction pattern of untreated, baked, and boiled bone. The peaks are identical for the three samples, indicating that there is no change in the crystal structure due to heating up to these temperatures. (B) Thermal gravimetric analysis of untreated bone and boiled. The weight loss shows the destruction of the organic matrix. The boiled bone loses less weight during the TGA experiment than the prebaked and untreated ones, suggesting a substantial weight loss during the pretreatment by boiling. The data have been normalized to a starting mass corresponding to the value at 234°C to eliminate variations due to differences in sample hydration. The curves for the two treatments are averages of four curves and three curves for the untreated and boiled samples, respectively. The arrow bars represent intersample variations by means of the standard deviation, showing that the difference between the two treatments is significant.

analysis of untreated and baked bone samples (data not shown) showed that baking at up to 200°C does not result in a change in the fraction of organic material, which is all lost above this temperature. The spread of the data in the graph gives an indication of the variability between samples, in total seven untreated and four boiled samples were tested. The samples used for Fig. 6B all came from one vertebra (four untreated, three boiled).

To assess the quality of the organic matrix, we used gel electrophoresis to look for extractable proteins. Fig. 7A shows the lanes for the untreated, boiled, and baked bone at 200°C, respectively. Fig. 7B shows the corresponding densitometry graphs. The untreated bone (lane 1) shows a

few dominant bands and several bands of lower intensity. The boiled bone (lane 2) shows generally fewer and weaker bands. The two high molecular weight bands around MW 300 (collagen type I triple helix) and the band at MW 65 (bovine serum albumin; BSA [38]) in the untreated samples are absent in the boiled sample and the bands around MW 200 are significantly less visible than in the untreated bone. The bands around MW 110 (type I collagen) that are partially merged in the untreated bone are well separated in the boiled sample. However, an additional band around MW 16 (possibly chondroitin and keratan sulfates) is present in the boiled bone. This could be either be an additional band that became extractable from

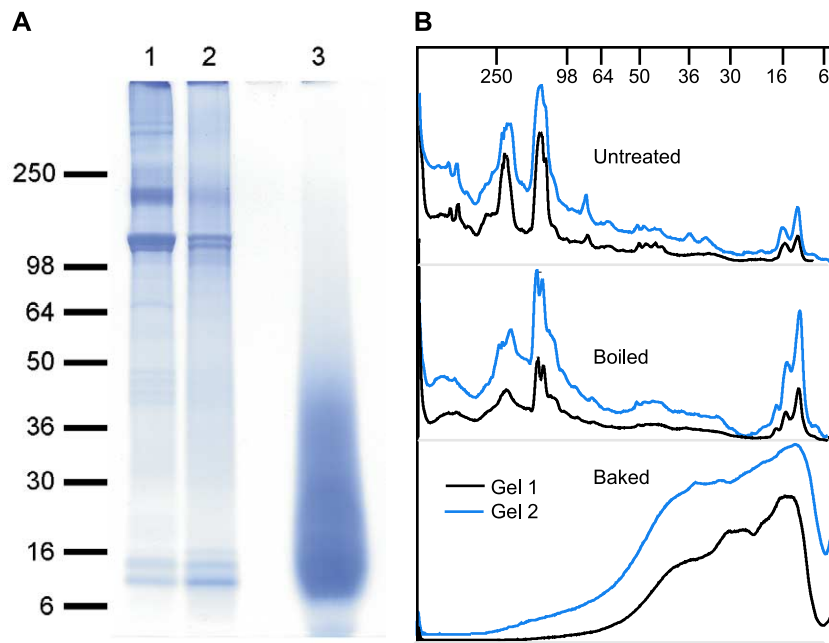


Fig. 7. Gel electrophoresis of proteins extracted from bone powder. (A) Gel electrophoresis of extracted proteins; lane 1: untreated bone; lane 2: boiled bone; lane 3: baked bone at 200°C for 40 min. (B) Densitometry of gels calibrated for optical density. The two traces per treatment represent two different samples that were representative for the five gels that were analyzed. The gels of different samples with same treatment correlate well.

the bone due to processes happening during boiling or could be fragments from other proteins that are denatured or decomposed due to the boiling. From the baked bone, however, no intact proteins could be extracted. From this and the TGA data, we can conclude that the organic in the bone is significantly degraded by baking, but not removed, whereas the boiling affects the nature of the organic constituents only slightly (gel results are very similar) but reduces the total amount of organic material (smaller weight loss in TGA).

Can the changes in the microscopic fracture behavior be correlated to macromechanical properties? To answer this question, we tested samples that were untreated, baked, or boiled in a custom-built mechanical impact tester, Fig. 1. The apparatus was designed to be able to exert forces at rates comparable to loading rates that occur during a fall of an adult human on the hip [39] (ca. 15 ms to peak force). The samples were successively loaded with an increase in peak force after every fourth hit. The forces that were applied to the sample and the compression of the sample were recorded. From this data, three interesting parameters could be extracted: (1) the maximum amount of accumulated energy that could be applied to the sample before it would break, (2) the rate of collapse before and after the sample has reached its yield point, and (3) the elastic compression of the samples during impact.

Fig. 8A shows the height of the samples after each hit. The baked and boiled samples both collapse under significantly less accumulated energy (summed impact energies over all hits) than the untreated samples, indicating a decrease in toughness. Furthermore, it can be seen that the baked bone collapses abruptly after it starts to yield, whereas the boiled and untreated bone retain part of their strength even after yielding. The height of the untreated bone is virtually unaffected by the lower energy impacts, whereas the height of the boiled and baked bone decreases already at low energy impacts. After impacts for a total 40 J of accumulated energy, the untreated bone has been permanently compressed by only 0.1%. The baked and the boiled samples, however, have at that accumulated energy been compressed by 1% (Fig. 8B).

Compression profiles during the impact are shown in Fig. 8C. The baked bone shows much less elasticity than the untreated and boiled bone. This again shows a decrease in toughness when the organic matrix in bone is degraded. The boiled bone collapses very gradually, suggesting a more elastic, deformable material. Several samples of each preparation were tested, extracted from two different vertebrae specimens.

Discussion

The microscopic fracture behavior of the bone samples under compression changes significantly with the pretreat-

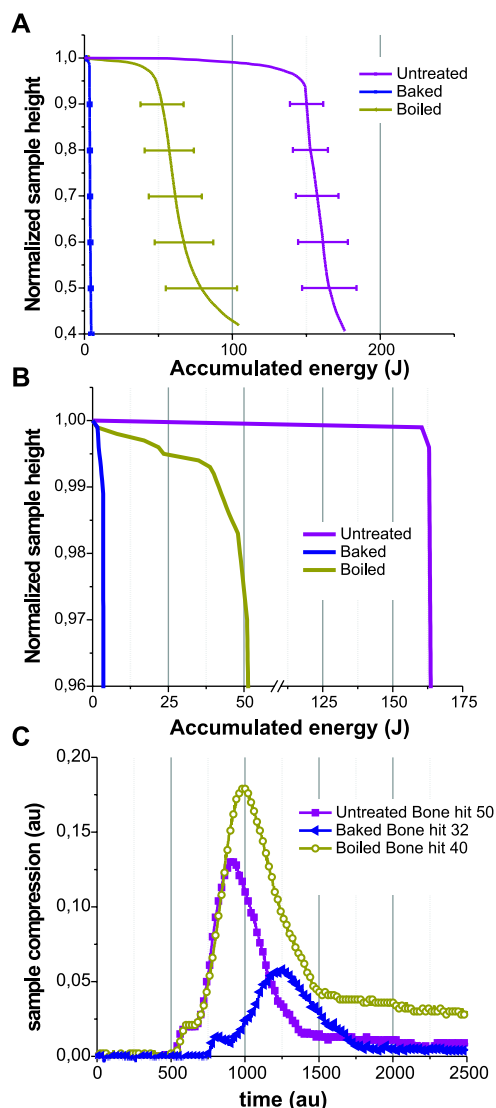


Fig. 8. Macroscopic fracture testing of the bone samples. (A) Normalized sample height after impacts, averaged over a total of 16 samples. The baked (200°C, 40 min) and the boiled (100°C, 2 h) bone samples have lost much of their strength compared to the untreated bone (they break at much lower accumulated impact energies). The collapse of the baked bone is very abrupt (indicating high brittleness) compared to the gradual collapse of the boiled bone that is tougher. Error bars represent 80% confidence regions due to sample variation. (B) Zoom in of low energy impact region on representative curves. The boiled bone sample shows significant permanent compression even at low impact energies. The untreated bone is much less affected by these low energy impacts and is hardly compressed at these soft impacts. (C) Compression profiles during impact of representative samples. The boiled bone samples are more compressible than the untreated samples. The baked samples are much less compressible. Curves represent hits close to the yield-accumulated energies of the samples.

ment of the organic matrix. Where the untreated matrix forms distinct fibrillar connections between the fractured surfaces (that have been reported to play an important role in the strength of bone [22]), the boiled bone shows thinner, less coherent filaments. The transition from “bulk-material” to the fibers is very gradual in these samples, suggesting the presence of mineral crystals in the denser regions of the

transition. The organic in the baked bone has lost its ability to form filaments completely, yielding fractures resembling those of a brittle material. This substantiates the theoretical predictions by Yeni and Norman [26] who have described the possible role of collagen fibers spanning a microcrack for the energy required for crack propagation.

The dominant fracture mechanism also depends to a large extent on the condition of the organic matrix. In the untreated and the boiled bone, delamination is the principal type of fracture, whereas in the baked bone the cracks are more random and are no longer oriented parallel to the trabecular surface.

The appearance of the surfaces changes significantly with the heat treatment. Baking the sample reveals very distinct fibers but removes the 67-nm banding typical for collagen. This indicates that this part of the organic matrix is degraded and can therefore no longer function as an energy-absorbing medium. It has been reported that in mouse models with osteogenesis imperfecta (OI), a type I collagen disorder that results in a deranged collagen matrix, bones are weaker, having reduced post yield deformation which is typical for brittle materials [40].

The surface of the boiled bone has a soft appearance, suggesting that the cohesion of the organic matrix is softened, but the organic is still present. This could explain the more flexible behavior of the boiled bone since the organic matrix no longer holds the inorganic components tightly together but is still important for energy dissipation.

The X-ray diffraction data show that none of our treatments have a significant effect on the inorganic phase, so the change in the fracture behavior has to be attributed to a change in the organic matrix or the interaction of the organic matrix with the mineral crystals. This is in good agreement with the findings of Rogers and Daniels [31] who have found no significant change in the X-ray diffraction pattern of bone heated to 200°C compared to native bone, and Catanese et al. [41] who have shown by X-ray diffraction that there is no change in the crystal structure when heating the bone as high as 350°C. Catanese et al. [41] have observed recrystallization in bone samples heated to 700°C whereas Rogers and Daniels report significant changes in the spectrum already between 400°C and 600°C.

From the TGA data, we know that at the temperatures the samples were baked, none of the organic was actually removed. This corresponds to the findings of Murugan et al. [33] who found that bone heated at 300°C showed the same peaks in the IR-spectrum as untreated bone. Catanese et al. [41] found that heating the bone up to 350°C removes 85% of the organic within a day of heating. Although there are different values in the literature for the temperature at which the bone starts to lose a significant part of its organic, all papers report only insignificant loss of organic from heating the bone to 200°C. The gel electrophoresis data, however, show that by heating the bone to 200°C, the extractable organic molecules have been significantly altered, indicating a significant change in the properties of the organic matrix.

The absence of the bands could indicate a destruction of the proteins or could be caused by a change in affinity of the proteins to the inorganic, altering the extractability of the proteins. Either of these changes could explain the absence of the filaments in the microcracks as seen by SEM. For the boiled bone, a slight change in the gel pattern is observed that might alter the influence of the organic matrix on the mechanical properties of the bone. In the TGA data, we see that bone has lost some of its organic during the boiling, which will also influence the contribution the organic matrix makes to the strength of bone. Although the effects of boiling of the bone is not directly related to physiological processes that occur in vivo, the boiling is a way to gently degrade the organic matrix by partially denaturing some of the proteins. Bone with partially degraded organic matrix by other treatments, such as irradiation, have also shown a reduction of the work to fracture. Currey et al. [42] report a reduction of the work to fracture that increases with increasing irradiation dose.

Macromechanically, the reduction in overall strength by heat-degrading the organic matrix shows once again the importance of the organic matrix being in healthy condition as has been reviewed by Currey [43]. Healthy bone not only requires more accumulated energy to be fractured, it is also much more resistant to low energy impacts than boiled bone. The fracture mechanism typical for a brittle material and the reduced reversible deformation of the baked bone shows that a highly degraded organic matrix results in brittle bone [40].

We have shown that degeneration of the organic matrix by heat has a large impact on the mechanical properties of bone. In healthy bone, the main failure mechanism is a delamination of the bone following the contours of the trabeculae, whereas in bone with the completely degraded organic (from baking), the main fracture type is rugged, nondirectional, diffuse crack propagation. In the boiled bone, the binding between the organic and the inorganic and the binding within the organic seems to be reduced, leading to a more flexible but less strong material. The bones with the completely degraded organic matrix were less strong in the macromechanical test than the untreated ones and showed less elastic deformation during the impacts. X-ray analysis shows that the inorganic components have not been affected by our heat treatments.

This, together with the altered crack formation, shows that the degradation of the organic matrix is responsible for the much more brittle nature of the degraded bone. Similar degradation of the organic, for example, aging of the organic matrix [44], could be a reason for the brittleness of older [45,46] or osteoporotic bone [47,48].

Acknowledgments

The authors thank Mark Cornish and Jan Lövdander from the Materials Research Laboratory Microscopy Facility for

instrumentation assistance and Herbert Waite, Sanje Wood-sorrel, Simcha Frieda Udwin, Marquesa Finch, and Manuella Venturoni for their support, suggestions, and fruitful discussions. This work was supported by the NSF Materials Research Department under grant Number DMR00-80034, NIH under grant number GM65354, NASA/URETI on Bio Inspired Materials under award number NCC-1-02037, a CNPq Fellowship (Brazil), and a research agreement with Veeco Instruments. HB thanks the Danish Natural Science Research Council for further financial support.

References

- [1] Weiner S, Traub W, Wagner HD. Lamellar bone: structure-function relations. *J Struct Biol* 1999;126:241–55.
- [2] Liu D, Wagner HD, Weiner S. Bending and fracture of compact circumferential and osteonal lamellar bone of baboon tibia. *J Mater Sci, Mater Med* 2000;11:49–60.
- [3] Reilly GC, Currey JD. The effects of damage and microcracking on the impact strength of bone. *J Biomech* 2000;33:337–43.
- [4] Wolff J. Über die innere architektur der knochen und ihre bedeutung für die frage vom knochenwachstum, *Archiv für pathologische Anatomie und Physiologie und für klinische Medizin*. Virchows Archiv 1870;50:389–453.
- [5] Müller R. The Zürich experience: one decade of three-dimensional high resolution computed tomography. *Top Magn Reson Imaging* 2002;13:307–22.
- [6] Silva MJ, Gibson LJ. Modeling the mechanical behavior of vertebral trabecular bone: effects of age-related changes in microstructure. *Bone* 1997;21:191–9.
- [7] Yeni YN, Norman TL. Fracture toughness of human femoral neck: effect of microstructure, composition and age. *Bone* 2000; 26:499–504.
- [8] Majumdar S, Kothari M, Augat P, Newitt DC, Link TM, Lin JC, et al. High-resolution magnetic resonance imaging: three-dimensional trabecular bone architecture and biomechanical properties. *Bone* 1998;22:445–54.
- [9] Thurner P, Wyss P, Obrist U, Sennhauser U, Müller R. Image guided fatigue assessment of bovine trabecular bone using synchrotron radiation (sr). *Trans-Eur Orthop Res Soc* 2003;13:14.
- [10] Aaron JE, Makins NB, Sagreya K. The microanatomy of trabecular bone loss in normal aging men and women. *Clin Orthop* 1987;215: 260–71.
- [11] Zioupos P. Accumulation of in-vivo fatigue microdamage and its relation to biomechanical properties in ageing human cortical bone. *J Microsc* 2001;201:270–8.
- [12] Zioupos P, Currey JD, Mirza MS, Barton DC. Experimentally determined microcracking around a circular hole in a flat plate of bone: comparison with predicted stresses. *Philos Trans, Biol Sci* 1995;347:383–96.
- [13] Weiner S, Wagner HD. The material bone: structure mechanical function relations. *Annu Rev Mater Sci* 1998;28:271–98.
- [14] Smith BL, Schaffer TE, Viani M, Thompson JB, Frederick NA, Kindt J, et al. Molecular mechanistic origin of the toughness of natural adhesives, fibres and composites. *Nature* 1999;399(6738):761–3.
- [15] Gao H, Ji B, Jäger IL, Arzt E, Fratzl P. Materials become insensitive to flaws at nanoscale: lessons from nature. *Proc Natl Acad Sci* 2003; 100:5597–600.
- [16] Thompson JB, Kindt JH, Drake B, Hansma HG, Morse DE, Hansma PK. Bone indentation recovery time correlates with bond reforming time. *Nature* 2001;414:773–6.
- [17] Rho JY, Kuhn-Spearing L, Zioupos P. Mechanical properties and the hierarchical structure of bone. *Med Eng Phys* 1998;20:92–102.
- [18] Wang X, Bank RA, TeKoppele JM, Hubbard GB, Althanasios KA, Agrawal CM. Effect of collagen denaturation on the toughness of bone. *Clin Orthop Relat Res* 2002;371:228–39.
- [19] Zioupos P, Currey JD, Hamer AJ. Role of collagen in the declining mechanical properties of ageing human cortical bone. *J Biomed Mater Res* 1999;45:108–16.
- [20] Jepsen KJ, Schaffler MB, Kuhn JL, Goulet RW, Bonadio J, Goldstein SA. Type I collagen mutation alters the strength and fatigue behavior of mov13 cortical tissue. *J Biomech* 1997;30:1141–7.
- [21] Oxlund H, Barckman M, Ortoft G, Andreassen TT. Reduced concentrations of collagen cross-links are associated with reduced strength of bone. *Bone* 1995;17:365–71.
- [22] Nalla RK, Kinney JH, Ritchie RO. Mechanistic fracture criteria for the failure of human cortical bone. *Nat Mater* 2003;2:164–8.
- [23] Rubin MA, Jasiuk I, Taylor J, Rubin J, Ganey T, Apkarian RP. TEM analysis of the nanostructure of normal and osteoporotic human trabecular bone. *Bone* 2003;33:270–82.
- [24] Landis WJ. The strength of calcified tissue depends in part on the molecular structure and organization of its constituent mineral crystals in their organic matrix. *Bone* 1995;16:533–44.
- [25] Benezra Rosen V, Hobbs LW, Spector M. The ultrastructure of anorganic bovine bone and synthetic hydroxyapatites used as bone graft substitute materials. *Biomaterials* 2002;23:921–8.
- [26] Yeni YN, Fyhrie DP. Collagen-bridged microcrack model for cortical bone tensile strength. *ASME Bioeng Conf* 2001;50:293–4.
- [27] Currey JD, Brear K, Zioupos P. Effects of aging and changes in mineral content in degrading the toughness of human femora. *J Biomech* 1996;29:257–60.
- [28] Raspanti M, Guizzardi S, DePasquale V, Martini D, Ruggeri A. Ultrastructure of heat-deproteinated compact bone. *Biomaterials* 1994;15:433–7.
- [29] Dyson ED, Jackson CK, Whitehouse WJ. Scanning electron microscope studies of human trabecular bone. *Nature* 1970;225:957–9.
- [30] Ertz D, Gathercole LJ, Atkins EDT. Scanning probe microscopy of intrafibrillar crystallites in calcified collagen. *J Mater Sci, Mater Med* 1994;5:200–6.
- [31] Rogers KD, Daniels P. An X-ray diffraction study of the effects of heat treatment on bone mineral microstructure. *Biomaterials* 2002;23:2577–85.
- [32] Danielsen CC. Age-related thermal stability and susceptibility to proteolysis of rat bone collagen. *Biochem J* 1990;272:697–701.
- [33] Murugan R, Panduranga Rao K, Sampath Kumar TS. Heat-deproteinated xenogeneic bone from slaughterhouse waste: physico-chemical properties. *Bull Mater Sci* 2003;26:523–8.
- [34] Rem AI, Oosterhuis JA, Journee-De Korver HG, Van Den Berg TJTP, Keunen JEE. Temperature dependence of thermal damage to the sclera: exploring the heat tolerance of the sclera for transscleral thermotherapy. *Exp Eye Res* 2001;72:153–62.
- [35] Robinovitch SN, Hayes WC, McMahon TA. Prediction of femoral impact forces in falls on the hip. *Trans Am Soc Mech Eng* 1991;113:366–74.
- [36] Gutschmann T, Fantner GE, Venturoni M, Ekani-Nkodo A, Thompson JB, Kindt JH, et al. Evidence that collagen fibrils in tendons are inhomogeneously structured in a tubelike manner. *Biophys J* 2003; 84:2593–8.
- [37] Venturoni M, Gutschmann T, Fantner GE, Kindt JH, Hansma PK. Investigations into the polymorphism of rat tail tendon fibrils using atomic force microscopy. *Biochem Biophys Res Commun* 2003;303: 508–13.
- [38] Raif EM, Harmand M-F. Molecular interface characterization in human bone matrix. *Biomaterials* 1993;14:978–84.
- [39] Courtney AC, Hayes WC, Gibson LJ. Age-related differences in post-yield damage in human cortical bone: experiment and model. *J Biomech* 1999;29:1463–71.
- [40] Jepsen KJ, Goldstein SA, Kuhn J, Schaffler MB, Bonadio J. Type-I collagen mutation compromises the post-yield behavior of mov13 long bone. *J Orthop Res* 1996;14:493–9.

- [41] Catanese JI, Featherstone JDB, Keaveny TM. Characterization of the mechanical and ultrastructural properties of heat-treated cortical bone for the use as a bone substitute. *J Biomed Mater Res* 1999;45:327–36.
- [42] Currey JD, Foreman J, Laketic I. Effects of ionizing radiation on the mechanical properties of human bone. *J Orthop Res* 1997;15:111–7.
- [43] Currey JD. Role of collagen and other organics in the mechanical properties of bone. *Osteoporos Int* 2003;14:29–36.
- [44] Eyre DR, Dickson IR, Van Ness K. Collagen cross-linking in human bone and articular cartilage. *Biochem J* 1988;252:495–500.
- [45] Zioupos P, Currey JD. Changes in the stiffness, strength and toughness of human cortical bone with age. *Bone* 1998;22:57–66.
- [46] Oxlund H, Mosekilde L, Ortoft G. Reduced concentration of collagen reducible cross links in human trabecular bone with respect to age and osteoporosis. *Bone* 1996;19:479–84.
- [47] Wang A, Shen X, Li X, Mauli Argawal C. Age-related changes in the collagen network and toughness of bone. *Bone* 2002;31:1–7.
- [48] Ammann P, Rizzoli R. Bone strength and its determinants. *Osteoporos Int* 2003;14(Suppl 3):13–8.